

Theoretical Study of Bimolecular Reactions between Carbenium Ions and Paraffins: The Proposal of a Common Intermediate for Hydride Transfer, Disproportionation, Dehydrogenation, and Alkylation

Merce Boronat,[†] Pedro Viruela,[‡] and Avelino Corma^{*,†}

Instituto de Tecnología Química UPV-CSIC, Universidad Politécnica de Valencia, av/ dels Tarongers s/n, 46022 Valencia, Spain, and Departament de Química Física, Universitat de València, c/ Dr. 50, 46100 Valencia, Spain

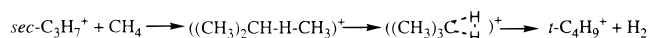
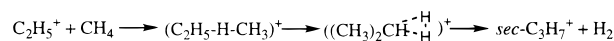
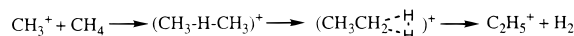
Received: March 22, 1999; In Final Form: June 11, 1999

The mechanism of the bimolecular reactions of ethyl cation with ethane and propane and of *s*-propyl cation with ethane, propane, and isopentane is theoretically investigated by means of the B3PW91 density functional method. The study includes complete geometry optimization and characterization of the reactants, products, reaction intermediates, and transition states involved, calculation of the reaction enthalpies and activation energies for the different elemental steps, and obtainment of the equilibrium constants and relative reaction rate constants by means of transition state theory. It is found that the interaction of a carbenium ion with a saturated alkane always results in formation of a stable carbonium ion intermediate and that different intramolecular rearrangements of this common intermediate can explain the mechanism of acid-catalyzed hydrocarbon reactions, such as hydride transfer, disproportionation, dehydrogenation, and alkylation.

1. Introduction

Carbonium ions are involved, as reaction intermediates or transition states, in the mechanism of many acid-catalyzed transformations of saturated hydrocarbons.¹ These nonclassical species are characterized by having a two-electron three-center bond and are formed by protonation of an alkane molecule or by addition of a carbenium ion to an alkane.

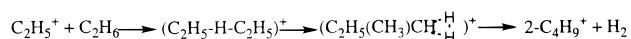
The existence of the smallest carbonium ions, CH₅⁺, C₂H₇⁺, C₃H₉⁺, *i*-C₄H₁₁⁺, and *n*-C₄H₁₁⁺ in the gas phase has been confirmed by mass spectrometry, and experimental^{2–6} and quantum chemical^{7–10} information concerning the structures and energetics of such systems has been reported. Hiraoka and Kebarle's gas-phase studies^{4,5} on the reaction of methane with methyl, ethyl, and *sec*-propyl carbenium ions indicated that C-protonated C₂H₇⁺, C₃H₉⁺, and *i*-C₄H₁₁⁺ carbonium ions are initially formed and rearrange to H-protonated isomers which dissociate into hydrogen plus the corresponding carbenium ion:



The potential energy surfaces of ethonium⁸ C₂H₇⁺, proponium⁹ C₃H₉⁺, and isobutonium¹⁰ *i*-C₄H₁₁⁺ cations have been extensively investigated, and it has been found that in order to obtain a good agreement between the calculated energies and experimental gas-phase data it is necessary to take into account electron correlation effects and zero-point energy corrections.

For the reactions of ethyl cations with ethane, Hiraoka and Kebarle¹¹ observed that the C-protonated *n*-C₄H₁₁⁺ carbonium

ion formed initially rearranges to the H-protonated form with an energy barrier of ~9.6 kcal/mol.

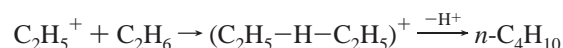


They estimated a value of ~13 kcal/mol for the stability of the (C₂H₅-H-C₂H₅)⁺ cation relative to separated C₂H₅⁺ + C₂H₆ and an exothermicity for the global process of ~21 kcal/mol. However, earlier studies¹² indicate that this reaction is exothermic only by 7 kcal/mol and that C₃H₇⁺ carbenium ions are also formed according to



with an enthalpy change of -9 kcal/mol. The only theoretical study of *n*-C₄H₁₁⁺ structures found in the literature^{9c} reveals that semiempirical methods and ab initio HF theory are inadequate to investigate this type of process, while MP2 and DFT correlated methods provide results comparable with each other.

The reactions of carbenium ions with saturated alkanes in liquid superacids such as HF-SbF₅ or FSO₃H-SbF₅ in low nucleophilicity media were widely investigated by Olah and his group in the 1960s and 1970s.¹³ They observed that, besides the degenerate hydride transfer reaction, other processes such as alkylation, dehydrogenation, and disproportionation also occur. It was then suggested that the different products obtained could be well explained by assuming ready intramolecular rearrangements of carbonium ion intermediates. For example, in the ethylation of ethane in HF-SbF₅/SO₂ClF media,¹³ a significant amount of *n*-butane is formed according to

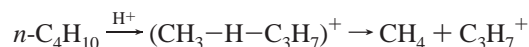


Other products observed in the system are *n*-hexanes formed by reaction of *n*-butane with excess C₂H₅⁺, and propane, which

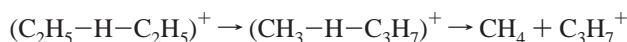
[†] Universidad Politécnica de Valencia.

[‡] Universitat de València.

can be formed either by secondary protolytic cleavages of *n*-butane

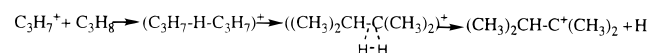
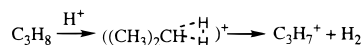


or by intramolecular rearrangement of the $\text{C}_4\text{H}_{11}^+$ carbonium ion intermediate



The direct alkylation reaction or deprotonation of a carbonium ion to give an alkane is hardly possible in the gas phase due to the absence of solvation effects and to the instability of the proton. However, it has been observed to occur both in solution^{13–15} and on solid acid catalysts such as HF-TaF_5 , $\text{HF-TaF}_5/\text{AlF}_3$, or $\text{HF-SbF}_5/\text{graphite}$.^{16,17}

In other cases,^{18,19} as for instance in the reactions of *sec*-propyl carbenium ion with propane, besides the intermolecular hydride transfer and the alkylation reactions, hydrogen evolution was observed in the system. The liberated H_2 comes from dehydrogenation of H-protonated forms of carbonium ions:



which in some cases results from isomerization of the C-protonated forms initially obtained.

More recently, some ^1H and ^2H NMR studies of the hydrogen–deuterium exchange between zeolite Y and 3-methylpentane²⁰ or isobutane²¹ also suggest that carbonium ions are formed and rearrange on the surface of zeolite catalysts. Thus, it is of great interest to understand the mechanism of formation, isomerization, and dissociation of carbonium ions.

We present in this paper a quantum chemical study of the bimolecular reactions between trivalent carbenium ions and saturated alkanes that occur through formation of carbonium ion intermediates. The systems considered are those formed by interaction of ethyl cation with ethane and propane, and of *sec*-propyl cation with ethane, propane, and isopentane. The study includes geometry optimization and characterization of all species involved in the mechanism (reactants, products, reaction intermediates, and transition states) and calculation of the reaction enthalpies and activation energies for the different reaction steps. Finally, equilibrium constants and reaction rate constants have been computed by means of the transition state theory (TST).²²

2. Computational Details

The present study is based on density functional theory,^{23,24} a methodology that allows for inclusion of the electron correlation at a much lower computational cost than traditional ab initio molecular orbital theory. The method used combines Becke's hybrid three-parameter exchange functional²⁵ that includes the Hartree–Fock exact exchange with the gradient-corrected correlation functional of Perdew and Wang²⁶ (B3PW91) and employs the standard 6-31G* basis set²⁷ that includes d-type polarization functions on nonhydrogen atoms. Previous studies²⁸ have shown that the results provided by the hybrid B3PW91 functional are in good agreement with experiment or with high-level ab initio calculations and that inclusion of polarization functions on hydrogen atoms does not significantly improve the results. The geometries of both minima and transition states have been fully optimized using the Berny analytical gradient method,²⁹ and the nature of every stationary point has been

TABLE 1: B3PW91/6-31G* Optimized Values of the Most Important Bond Lengths (in Å) of $\text{C}_4\text{H}_{11}^+$ Species^a

	C ₁ –C ₂	C ₂ –C ₃	C ₃ –C ₄	C ₁ –H ₁	C ₂ –H ₁	C ₃ –H ₁	C ₂ –H ₂
M1	1.489	2.438	1.489		1.261	1.261	
TS1	1.694	1.690	1.523	1.528	1.134	1.600	
M2	2.374	1.478	1.562	1.184	1.373		
TS2	2.715	1.431	1.607	1.132	1.696		
M3	3.490	1.398	1.674	1.095	3.106		
TS3	1.523	1.630	1.521		1.172	1.731	1.194
M4	1.519	1.535	1.525		1.300		1.273
TS4	1.503	1.500	1.526		1.505		1.457

^a The atomic numbering is given in Figure 1.

TABLE 2: B3PW91/6-31G* Optimized Values of the Most Important Bond Lengths (in Å) of $\text{C}_5\text{H}_{13}^+$ Species^a

	C ₁ –C ₂	C ₂ –C ₃	C ₃ –C ₄	C ₁ –H ₁	C ₂ –H ₁	C ₃ –H ₁
M5	1.492	2.426	1.492		1.254	1.272
TS5	1.520	2.932	1.418		1.123	1.927
M6	1.527	3.276	1.400		1.102	2.654
TS6	1.702	1.678	1.532	1.516	1.136	1.605
M7	2.462	1.463	1.584	1.173	1.423	
TS7	2.691	1.432	1.616	1.139	1.639	
TS8	1.521	1.633	1.536		1.704	1.171
M8	1.497	2.563	1.486		1.203	1.372
TS9	1.523	1.690	1.698		1.529	1.160
TS10	1.716	1.705	1.523	1.507	1.128	1.671
M9	2.468	1.465	1.523	1.167	1.446	
TS11	2.632	1.440	1.519	1.143	1.600	
TS12	1.525	1.642	1.527		1.633	1.180

^a The atomic numbering is given in Figures 2 and 3.

characterized by calculating the Hessian matrix and analyzing the vibrational normal modes. Zero-point vibrational corrections (ZPE) to the total energies and standard state enthalpies for comparison with experimental data have also been obtained from the frequency calculations.

Using the computed reaction enthalpies, activation barriers and partition functions of reactants, products, and transition states, we have calculated equilibrium and relative reaction rate constants by means of the transition state theory (TST).²² The equilibrium constant is calculated according to

$$K_c = \prod_i \left(\frac{z_i}{VN_A} \right)^{\nu_i} \exp(-\Delta E_0/RT)$$

and the relative rate constant for two reactions is given by

$$\frac{k_1}{k_2} = \frac{z_{\text{TS1}}}{z_{\text{TS2}}} \exp((E_{0(\text{TS2})} - E_{0(\text{TS1})})/RT)$$

where T is the temperature (298.15 K), E_0 is the energy which includes the zero-point vibrational correction ($E_0 = E + \text{ZPE}$), and z is the partition function which takes into account entropic effects.

All calculations have been performed on SGI Power Challenge workstations using the Gaussian 94 computer program.³⁰

3. Results and Discussion

The calculated structures and relative energies corrected for the zero-point vibrational contribution (ZPE) of all the $\text{C}_4\text{H}_{11}^+$, $\text{C}_5\text{H}_{13}^+$, $\text{C}_6\text{H}_{15}^+$, and $\text{C}_8\text{H}_{19}^+$ species studied and the reaction paths in which they are involved are shown in Figures 1–7. Their most important optimized geometric parameters are listed in Tables 1–4, and Table 5 summarizes the standard state reaction enthalpies and equilibrium constants calculated for the different processes investigated in this work.

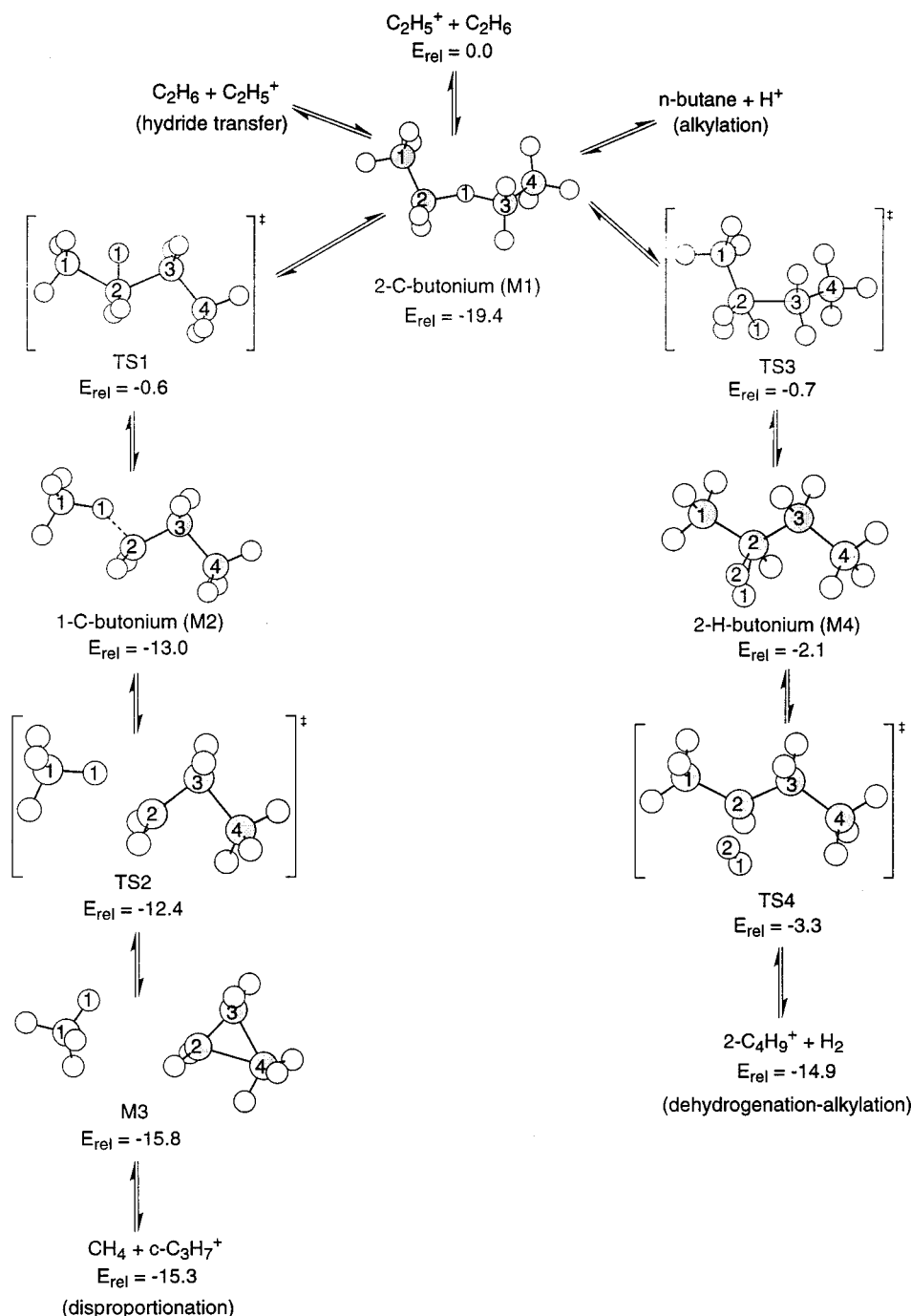


Figure 1. Reaction paths in which the 2-C-butionium intermediate is involved and B3PW91/6-31G* calculated relative energies (with ZPE corrections) in kcal/mol.

$\text{C}_2\text{H}_5^+ + \text{C}_2\text{H}_6$. Addition of ethyl cation to ethane results in formation of the stable 2-C-butionium carbonium ion (M1 in Figure 1). This process was theoretically studied at the ab initio MP2 level,³¹ and a weak ion-molecule complex that rearranged into 2-C-butionium with a small activation barrier of 0.4 kcal/mol was localized. At the B3PW91/6-31G* level, however, no weak complex has been found and interaction of ethyl cation with ethane directly yields structure M1 without activation energy. It should be mentioned that this failure of density functional theory to accurately evaluate weak van der Waals interactions has already been observed and reported in the literature.³² The optimized geometry of M1, summarized in Table 1, corresponds to a species having a symmetrical closed two-electron three-center bond, with the calculated C-H-C angle value being 150.2°. The nature of the 2-C-butionium ion

has been characterized by a frequency calculation, and it has been found to be a minimum of 19.4 kcal/mol with the ZPE correction more stable than separated ethyl and ethane.

As shown in Figure 1, 2-C-butionium is the key intermediate in the mechanism of four different acid-catalyzed hydrocarbon reactions. One of the processes is the already studied hydride transfer between alkanes and alkylcarbenium ions, which involves backward decomposition of M1 into ethane and ethyl cation. If instead of decomposing the 2-C-butionium gives the proton of its C-H-C bond back to the catalyst, the obtained product is a butane molecule and the process is an alkylation reaction. This step cannot be studied theoretically unless the catalyst and the solvent are explicitly considered in the calculations and, as told in the Introduction, it can hardly occur in the gas phase due to the absence of solvation effects and to

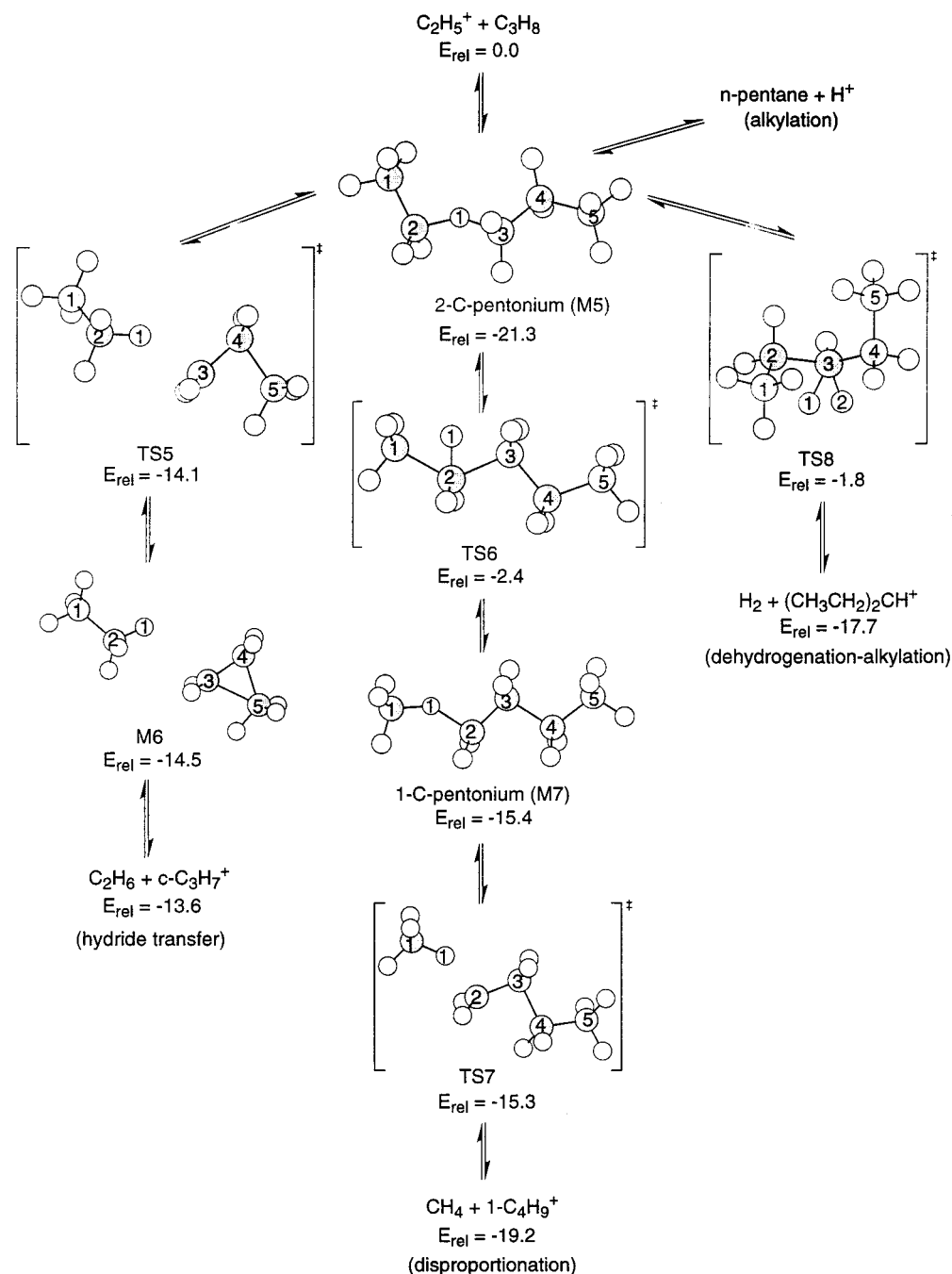


Figure 2. Reaction paths in which the 2-C-pentonium intermediate is involved and B3PW91/6-31G* calculated relative energies (with ZPE corrections) in kcal/mol.

the instability of the proton as compared to other carbenium ions. However, it is of special importance since it represents a mechanism for the alkane-alkene alkylation which is completely different from that generally accepted. Indeed, the classical mechanism for alkylation of paraffins with olefins³³ is a chain mechanism in which the initiation step is protonation of the olefin, followed by hydride transfer from a reactant alkane to the initial carbenium ion intermediate. In a following step, the new carbenium ion attacks an olefin to give the corresponding alkylated carbenium ion which by abstraction of a hydride ion from an alkane reactant yields the alkylated product. Our results show that a paraffin can be directly alkylated by a carbenium ion through the formation of a carbonium ion intermediate, as has been proposed to occur in superacid media.¹³⁻¹⁵

The third process considered here starts with conversion of

the 2-C-butyronium ion (M1) into the 1-C-butyronium ion (M2) through transition state TS1. 1-C-butyronium has also a closed two-electron three-center bond with a calculated C-H-C angle value of 136.3°, but due to the different nature of the two carbon atoms involved, the bond is not symmetrical and the bridged hydrogen atom is closer to C₁ than to C₂. The frequency calculation performed for 1-C-butyronium indicates that it is a minimum of 6.4 kcal/mol less stable than 2-C-butyronium. It is important to note that both $\text{C}_4\text{H}_{11}^+$ isomers were investigated by Collins and O'Malley at several semiempirical, ab initio, and density functional levels^{9c} and that our B3PW91/6-31G* results are in complete agreement with those obtained using the more expensive correlated ab initio MP2 method. In the transition state TS1, the C₁-C₂ and C₂-C₃ optimized bond length values are similar and the hydrogen atom that migrates from one C-C bond to the other one is approximately halfway

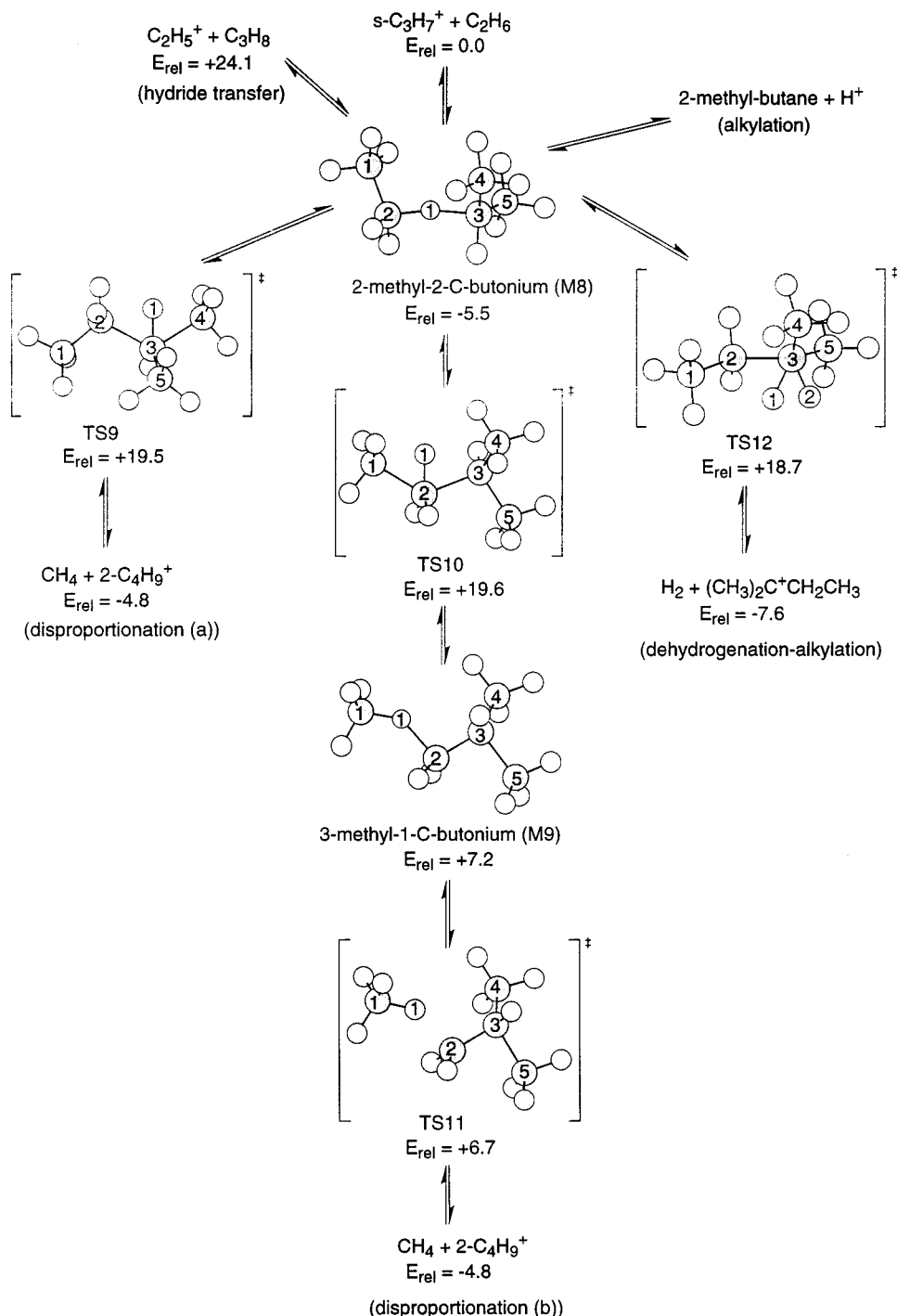


Figure 3. Reaction paths in which the 2-methyl-2-C-butonium intermediate is involved and B3PW91/6-31G* calculated relative energies (with ZPE corrections) in kcal/mol.

between C_1 and C_3 . The only imaginary vibrational mode obtained from the frequency calculations, of 861 i cm^{-1} , is clearly associated with the movement of the hydrogen atoms between the two C—C bonds. The calculated activation energy for conversion of 2-C-butonium into 1-C-butonium is 18.8 kcal/mol, and 12.4 kcal/mol for the reverse process.

It can be seen in Figure 1 that dissociation of 1-C-butonium yields methane and cyclopropyl cation, a species which has been confirmed to be a minimum on the C_3H_7^+ potential energy surface.³⁴ The reaction path involves rearrangement of M2 into a weak complex between CH_4 and $\text{c-C}_3\text{H}_7^+$ (M3) via transition state TS2 with an activation barrier of only 0.6 kcal/mol. The optimized parameters listed in Table 1 indicate that in TS2 there is still a strong interaction between the methane and the propyl

fragments, reflected both in the stretching of the $\text{C}_1\text{—H}_1$ bond and in the fact that the $\text{C}_1\text{—C}_2$ distance is not much longer than the $\text{C}_2\text{—C}_4$ one. However, in M3, which is only 0.5 kcal/mol more stable than separated products, the $\text{C}_1\text{—C}_2$ distance is quite long and the rest of the optimized values are similar to those calculated for isolated methane and c-propyl cation. The global process, which starts by the attack of ethyl cation to ethane and yields methane and c-propyl cation as products, is therefore a disproportionation reaction, which can lead by desorption or hydride transfer to a product with more carbon atoms than the starting reactants.

The last process in which 2-C-butonium (M1) is involved starts with its conversion, via transition state TS3, into the 2-H-

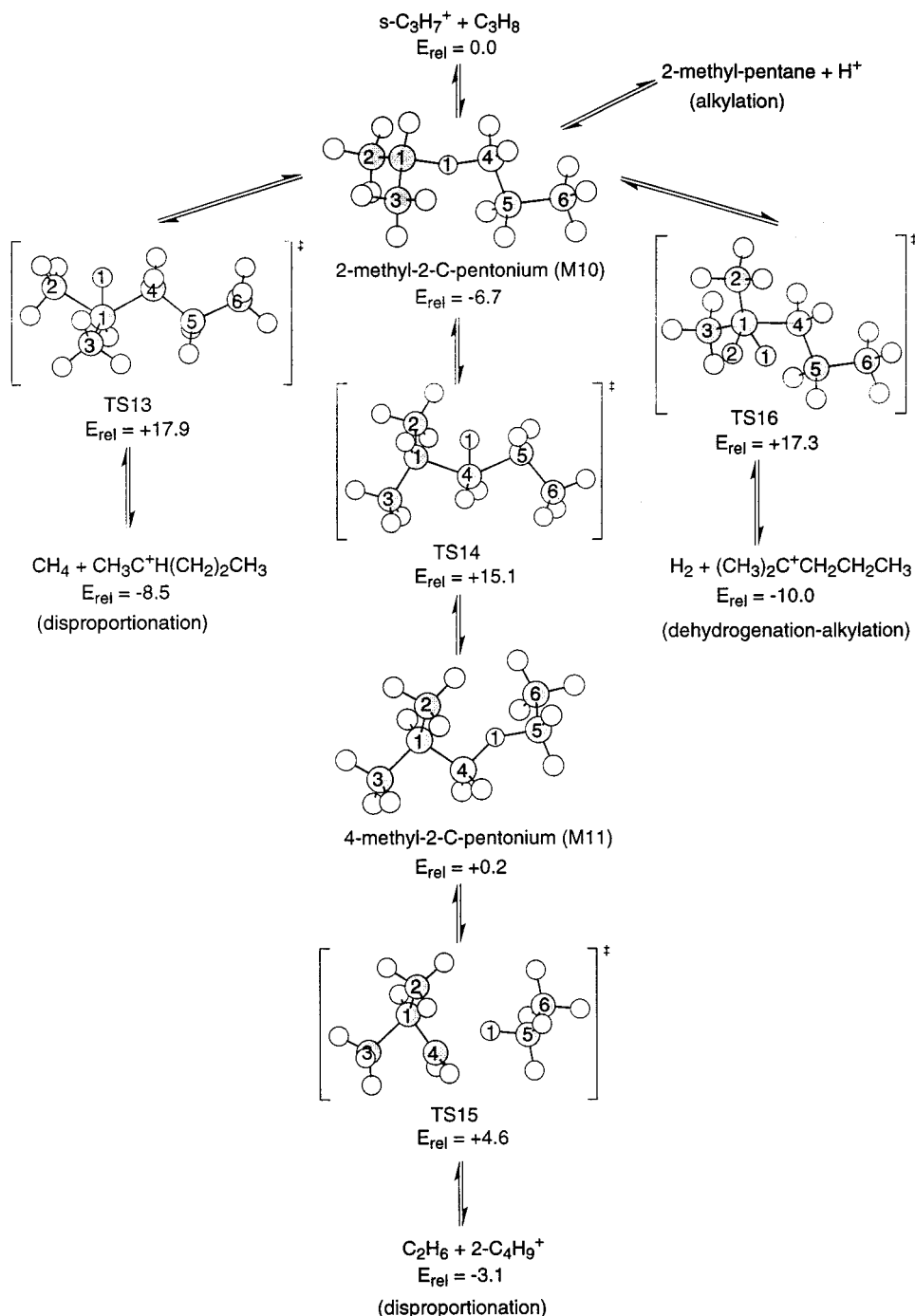


Figure 4. Reaction paths in which the 2-methyl-2-C-pentonium intermediate is involved and B3PW91/6-31G* calculated relative energies (with ZPE corrections) in kcal/mol.

butonium cation (M4), which has also been characterized as a minimum on the $n\text{-C}_4\text{H}_{11}^+$ potential energy surface. The $\text{C}_2\text{—H}_1$ and $\text{C}_2\text{—H}_2$ calculated bond length values in M4, listed in Table 1, are longer than normal C—H bonds, and the $\text{H}_1\text{—H}_2$ distance, 0.855 Å, is not much longer than the calculated value for molecular hydrogen, indicating that this structure has a two-electron three-center bond between C_2 , H_1 , and H_2 . Although there are no experimental data concerning the energetics of $n\text{-C}_4\text{H}_{11}^+$ isomers in the gas phase, it has been observed both in superacid media³⁵ and on acidic zeolites³⁶ that n -butane and other linear alkanes preferentially undergo C—C rather than C—H bond protolysis. In agreement with these experimental observations, 2-H-butionium (M4) has been calculated to be 17.3 kcal/mol less stable than 2-C-butionium, and 10.9 kcal/mol less stable than 1-C-butionium. The calculated activation barrier for

conversion of 2-C-butionium into 2-H-butionium via TS3 is 18.7 kcal/mol. This barrier is higher than the experimental value of 9.6 kcal/mol reported by Hiraoka and Kebarle,¹¹ due in part to the difference between the calculated and the experimental stability of 2-C-butionium. The only imaginary vibrational mode obtained for TS3, of 527i cm^{-1} , is mainly associated with the movement of the bridged hydrogen atom out of the C—C bond. Finally, it can be seen in Figure 1 that 2-H-butionium is not stable with respect to dissociation and decomposes into molecular hydrogen and the open or methyl-bridged form of the 2-butyl carbenium ion through transition state TS4. This structure is 0.5 kcal/mol less stable than M4 if the zero-point vibrational energy is not included. However, if the ZPE is taken into account, the transition state becomes more stable than the minimum, indicating that the potential energy surface in this

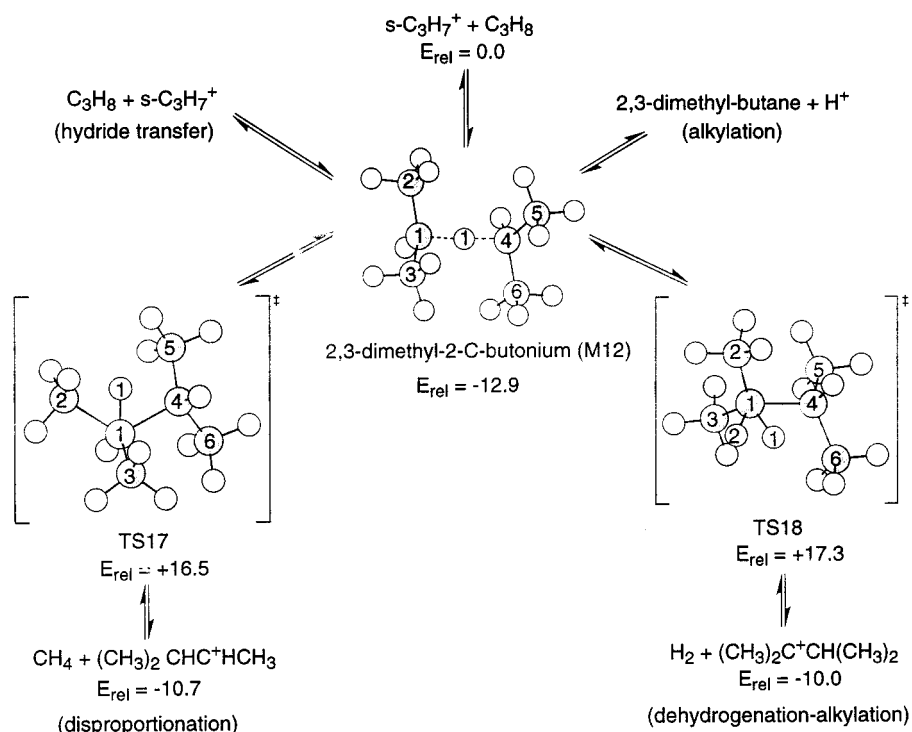


Figure 5. Reaction paths in which the 2,3-dimethyl-2-C-butonium intermediate is involved and B3PW91/6-31G* calculated relative energies (with ZPE corrections) in kcal/mol.

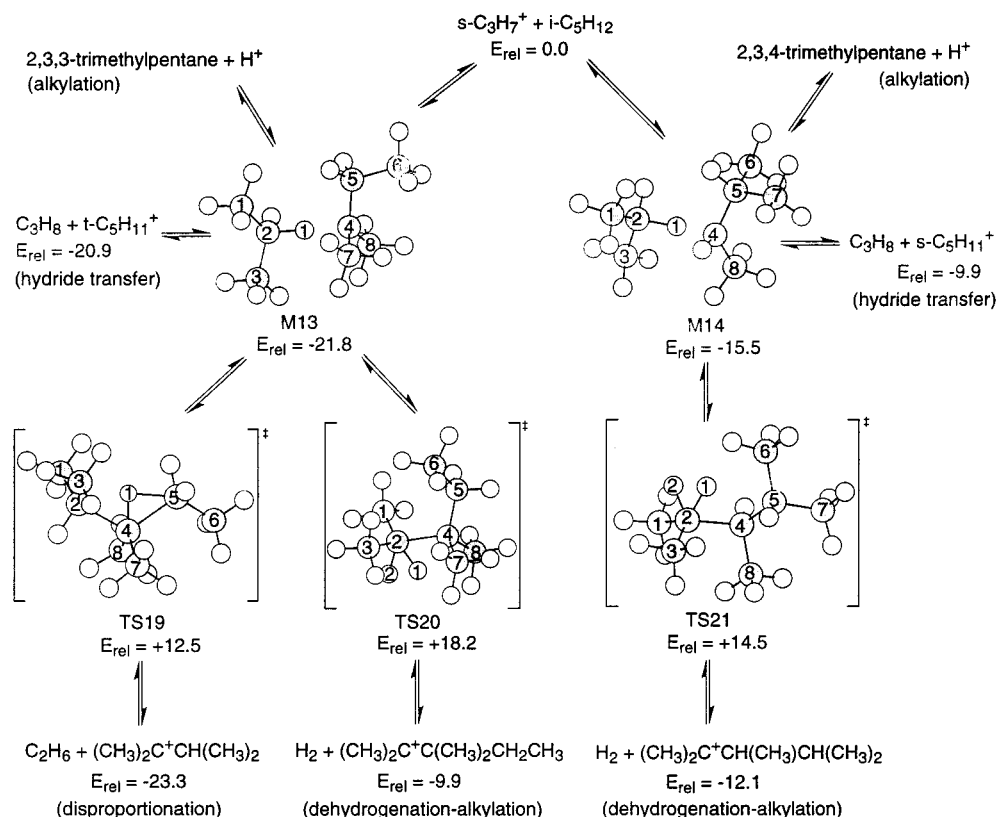


Figure 6. Reaction paths in which the carbonium ion intermediates formed by addition of $s\text{-C}_3\text{H}_7^+$ cation to the tertiary and secondary C–H bonds of isopentane are involved and B3PW91/6-31G* calculated relative energies (with ZPE corrections) in kcal/mol.

region is very flat. Since one of the products obtained by following this path is a hydrogen molecule, the global process is a dehydrogenation reaction; but since the other product (2-C₄H₉⁺ cation) is a species with the same number of carbon atoms than the sum of the carbon atoms of the initial reactants, the total process can also be considered as an alkylation.

Experimental evidence for this type of alkylation reaction in which hydrogen gas is liberated was provided by Olah^{18,19} in superacid media and has also been observed to occur in the gas phase.^{6a,b}

As shown in Table 5, the calculated enthalpies for the disproportionation and the dehydrogenation–alkylation reactions

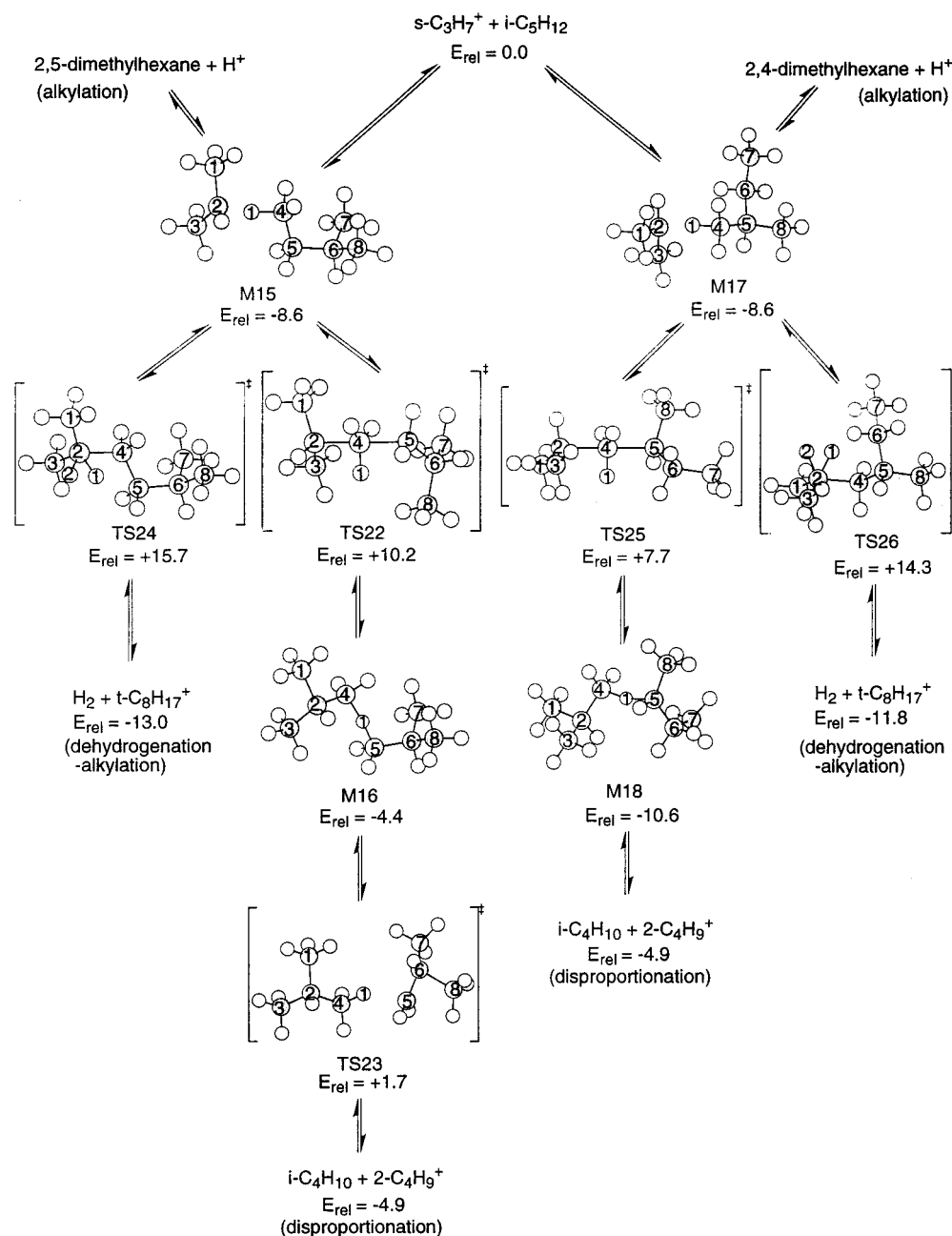


Figure 7. Reaction paths in which the carbonium ion intermediates formed by addition of $s\text{-C}_3\text{H}_7^+$ cation to the primary C–H bonds of isopentane are involved and B3PW91/6-31G* calculated relative energies (with ZPE corrections) in kcal/mol.

TABLE 3: B3PW91/6-31G* Optimized Values of the Most Important Bond Lengths (in Å) of $\text{C}_6\text{H}_{15}^+$ Species^a

	C ₁ –C ₂	C ₁ –C ₃	C ₁ –C ₄	C ₄ –C ₅	C ₁ –H ₁	C ₄ –H ₁
M10	1.490	1.489	2.533	1.500	1.354	1.211
TS13	1.703	1.514	1.683	1.531	1.161	1.534
TS14	1.518	1.520	1.735	1.764	1.758	1.108
M11	1.526	1.558	1.494	2.416		1.285
TS15	1.515	1.636	1.425	2.826		1.770
TS16	1.528	1.527	1.637	1.531	1.185	1.633
M12	1.496	1.496	2.543	1.496	1.276	1.276
TS17	1.710	1.513	1.721	1.534	1.147	1.579
TS18	1.528	1.527	1.670	1.525	1.181	1.637

^a The atomic numbering is given in Figures 4 and 5.

are -15.0 and -13.9 kcal/mol, respectively. The experimental gas-phase values reported by Blair et al.¹² are not so large, -9 and -7 kcal/mol, respectively, but as previously discussed, there are discrepancies between the experimental gas-phase reaction energies reported by different authors. The conclusion that can

TABLE 4: B3PW91/6-31G* Optimized Values of the Most Important Bond Lengths (in Å) of $\text{C}_8\text{H}_{19}^+$ Species^a

	C ₂ –C ₄	C ₄ –C ₅	C ₂ –H ₁	C ₄ –H ₁	
M13	2.632	1.502	1.200	1.434	$\angle\text{C}_2\text{–H}_1\text{–C}_4 = 175.5^\circ$
TS19	1.756	1.779	1.562	1.147	1.447
TS20	1.690	1.545	1.190	1.659	$r\text{C}_2\text{–H}_2 = 1.214$
M14	2.577	1.506	1.256	1.308	$\angle\text{C}_2\text{–H}_1\text{–C}_4 = 171.5^\circ$
TS21	1.666	1.551	1.195	1.692	$\text{C}_2\text{–H}_2 = 1.187$
M15	2.543	1.493	1.339	1.219	$\angle\text{C}_2\text{–H}_1\text{–C}_4 = 167.3^\circ$
TS22	1.765	1.875	2.116	1.089	$\text{C}_5\text{–H}_1 = 2.101$
M16	1.493	2.517		1.273	$\text{C}_5\text{–H}_1 = 1.267$
TS23	1.528	2.813		1.131	$\text{C}_5\text{–H}_1 = 1.824$
TS24	1.634	1.533	1.188	1.630	$\text{C}_2\text{–H}_2 = 1.200$
M17	2.533	1.500	1.334	1.223	$\angle\text{C}_2\text{–H}_1\text{–C}_4 = 164.2^\circ$
TS25	1.838	1.864	2.145	1.085	$\text{C}_5\text{–H}_1 = 2.151$
M18	1.505	2.553		1.208	$\text{C}_5\text{–H}_1 = 1.368$
TS26	1.635	1.535	1.193	1.652	$\text{C}_2\text{–H}_2 = 1.187$

^a The atomic numbering is given in Figures 6 and 7.

be obtained from these values is that both reactions are exothermic, with their reaction enthalpies being similar. When

TABLE 5: B3PW91/6-31G* Calculated Standard State Reaction Enthalpies (kcal/mol) and Equilibrium Constants ($T = 298.15$ K)^a

	ΔH°	K_c
$C_2H_5^+ + C_2H_6 \leftrightarrow CH_4 + c\text{-}C_3H_7^+$	-15.0	7.5×10^{10}
$C_2H_5^+ + C_2H_6 \leftrightarrow H_2 + 2\text{-}C_4H_9^+$	-13.9	2.7×10^7
$C_2H_5^+ + C_3H_8 \leftrightarrow C_2H_6 + c\text{-}C_3H_7^+$	-13.4	9.2×10^9
$C_2H_5^+ + C_3H_8 \leftrightarrow CH_4 + 1\text{-}C_4H_9^+$	-18.8	2.0×10^{13}
$C_2H_5^+ + C_3H_8 \leftrightarrow H_2 + 3C_5H_{11}^+$	-16.4	8.8×10^8
$C_2H_5^+ + C_3H_8 \leftrightarrow C_2H_6 + s\text{-}C_3H_7^+$	-23.6	5.4×10^{17}
$s\text{-}C_3H_7^+ + C_2H_6 \leftrightarrow CH_4 + 2\text{-}C_4H_9^+$	-4.7	5.2×10^2
$s\text{-}C_3H_7^+ + C_2H_6 \leftrightarrow H_2 + t\text{-}C_5H_{11}^+$	-6.7	3.0×10^1
$s\text{-}C_3H_7^+ + C_3H_8 \leftrightarrow CH_4 + 2\text{-}C_5H_{11}^+$	-8.3	9.8×10^4
$s\text{-}C_3H_7^+ + C_3H_8 \leftrightarrow C_2H_6 + 2\text{-}C_4H_9^+$	-3.2	1.0×10^2
$s\text{-}C_3H_7^+ + C_3H_8 \leftrightarrow H_2 + (CH_3)_2C^+(CH_2)_2CH_3$	-8.9	5.3×10^2
$s\text{-}C_3H_7^+ + C_3H_8 \leftrightarrow CH_4 + s\text{-}C_5H_{11}^+$	-10.3	3.5×10^6
$s\text{-}C_3H_7^+ + C_3H_8 \leftrightarrow H_2 + (CH_3)_2C^+CH(CH_3)_2$	-9.0	5.0×10^2
$s\text{-}C_3H_7^+ + i\text{-}C_5H_{12} \leftrightarrow C_3H_8 + t\text{-}C_5H_{11}^+$	-20.8	2.6×10^{15}
$s\text{-}C_3H_7^+ + i\text{-}C_5H_{12} \leftrightarrow H_2 + (CH_3)_2C^+C(CH_3)_2CH_2CH_3$	-8.7	1.4×10^2
$s\text{-}C_3H_7^+ + i\text{-}C_5H_{12} \leftrightarrow C_2H_6 + (CH_3)_2C^+CH(CH_3)_2$	-23.1	4.3×10^{16}
$s\text{-}C_3H_7^+ + i\text{-}C_5H_{12} \leftrightarrow C_3H_8 + s\text{-}C_5H_{11}^+$	-9.9	1.8×10^7
$s\text{-}C_3H_7^+ + i\text{-}C_5H_{12} \leftrightarrow H_2 + (CH_3)_2C^+CH(CH_3)CH(CH_3)_2$	-10.9	5.7×10^3
$s\text{-}C_3H_7^+ + i\text{-}C_5H_{12} \leftrightarrow i\text{-}C_4H_{10} + 2\text{-}C_4H_9^+$	-5.2	6.1×10^3
$s\text{-}C_3H_7^+ + i\text{-}C_5H_{12} \leftrightarrow H_2 + (CH_3)_2C^+(CH_2)_2CH(CH_3)_2$	-11.9	3.1×10^4
$s\text{-}C_3H_7^+ + i\text{-}C_5H_{12} \leftrightarrow H_2 + (CH_3)_2C^+CH_2CH(CH_3)CH_2CH_3$	-10.7	3.9×10^3

^a A table with the absolute energies (hartrees), ZPE, $H^\circ(298\text{ K}) - H^\circ(0\text{ K})$, absolute entropies, and total partition function (total, relative to the first vibrational state ($\nu = 0$)) is available on request from the authors.

the entropic effects are taken into account, the disproportionation reaction becomes more favored than the dehydrogenation-alkylation one, as reflected in the fact that the equilibrium constant calculated for the dehydrogenation reaction is 3 orders of magnitude lower than the disproportionation value.

With regards to kinetic information, from a study of the reactions of H_3^+ with neutral reactants,^{6c} a value of 1.4×10^{-12} s⁻¹ for the disproportionation and of 9×10^{-12} cm³ molecule⁻¹ s⁻¹ for the dehydrogenation-alkylation reactions were deduced. Our theoretical study of the $C_4H_{11}^+$ potential energy surface indicates that both processes start with formation of the 2-C-butionium intermediate by addition of ethyl cation to ethane. The rate-determining step for the disproportionation reaction is conversion of M1 into M2 through transition state TS1, while the rate-determining step for the dehydrogenation reaction is conversion of M1 into M4 via transition state TS3. This allows us to calculate the relative reaction rate $k_{\text{disproportionation}}/k_{\text{dehydrogenation}}$ as

$$\frac{k_{\text{disproportionation}}}{k_{\text{dehydrogenation}}} = \frac{z_{\text{TS1}}}{z_{\text{TS3}}} \exp((E_{0(\text{TS3})} - E_{0(\text{TS1})})/RT)$$

The calculated value, 0.9, indicates that both reactions are equally fast, in agreement with the experimental observations.

$C_2H_5^+ + C_3H_8$. Since propane has both primary and secondary C-H bonds, it can yield by interaction with ethyl cation two different carbonium ion intermediates: 2-C-pentonium (M5 in Figure 2) and 2-methyl-2-C-butionium (M8 in Figure 3). The different nature of the carbon atoms involved in the nonclassical 2e-3c bonds existing in M5 (primary-primary) and M8 (primary-secondary) is reflected in the optimized geometries and in the relative energies of both structures. Thus, while the C-H-C bond angle in M5 is closed, with a $C_2\text{-H}_1\text{-C}_3$ calculated angle value of 147.6°, and nearly symmetrical, in M8, it is almost linear, with a calculated angle value of 168.9°, and markedly asymmetrical. From the relative energies given in Figures 2 and 3, it can be deduced that 2-methyl-2-C-butionium (M8) is 8.3 kcal/mol more stable than 2-C-pentonium (M5).

The reaction paths for which 2-C-pentonium (M5) is the common intermediate, which are going to be discussed first,

are depicted in Figure 2. It can be seen that, like 2-C-butionium, 2-C-pentonium can donate the proton of its C-H-C bond back to the catalyst yielding *n*-pentane as the product of a direct alkylation reaction. The reaction path for the hydride transfer process is more complicated and yields as products ethane and *c*-propyl cation. It involves rearrangement of 2-C-pentonium (M5) into a weak complex between C_2H_6 and $c\text{-}C_3H_7^+$ (M6) through transition state TS5, with an activation energy of 7.2 kcal/mol. It can be seen in Table 2 that the $C_2\text{-H}_1$ bond is more stretched and the $C_2\text{-C}_3$ and $C_3\text{-H}_1$ calculated distances are shorter in TS5 than in M6. This indicates that while the interaction between the ethane and the propyl fragments in the transition state is still strong, in M6 this interaction is weak, as reflected also in the fact that it is only 0.9 kcal/mol more stable than separated products.

In the next process studied, the bridged proton moves from a central C-C bond to an outer one, and 2-C-pentonium (M5) is converted into 1-C-pentonium (M7) through transition state TS6 with an activation energy of 18.9 kcal/mol. The optimized geometry of TS6 is similar to that of TS1 in Figure 1. The $C_1\text{-C}_2$ and $C_2\text{-C}_3$ bond lengths are equivalent, the $C_2\text{-H}_1$ bond is stretched, and the hydrogen atom that is migrating, H_1 , is approximately at the same distance from C_1 than from C_3 . This structure has been characterized by a frequency calculation as a transition state, and the only imaginary vibration mode obtained, of 864i cm⁻¹, is clearly associated with the movement of H_1 from one C-C bond to the other one. 1-C-pentonium (M7), which has been characterized as a minimum on the potential energy surface, has a nonclassical asymmetrical closed 2e-3c bond between a primary and a methane carbon atoms, and therefore it has been calculated to be 5.9 kcal/mol less stable than 2-C-pentonium. Dissociation of 1-C-pentonium via transition state TS7 with a calculated activation energy of only 0.1 kcal/mol yields as products methane and the 1-butyl carbenium ion, with the global process being a disproportionation reaction. It is important to remark at this point that the 1-butyl carbenium ion obtained by dissociation of M7 is a minimum only 9.7 kcal/mol higher in energy than the 2-butyl carbenium ion, in agreement with previously reported ab initio calculations.³⁷

Finally, 2-C-pentonium can be dehydrogenated via transition state TS8 yielding molecular hydrogen and the linear 3- $C_5H_{11}^+$

carbenium ion, with an activation energy of 19.5 kcal/mol. The optimized values of the C₃–H₁ and C₃–H₂ distances in TS8, listed in Table 2, are longer than normal C–H bond lengths, while the calculated H₁–H₂ distance, 1.010 Å, is quite short. The only imaginary vibrational mode obtained from the frequency calculation performed for TS8, of 727i cm⁻¹, is clearly associated with the movement of H₁ out of the C₂–C₃ bond and toward H₂. Since we previously found that 2-H-butionium carbonium ion (M4) is not stable with respect to dissociation and that the potential energy surface in this region is quite flat, we have not investigated the existence or not of a minimum between TS8 and the reaction products. In this way, the reaction path is simplified, while no important information concerning the energetics or kinetics of the reaction is lost.

It can be observed in Table 5 that all the reactions of ethyl cation with propane investigated are exothermic and have large equilibrium constants. The thermodynamically most favorable process is the hydride transfer that, through formation of the 2-methyl-2-C-butionium (M8) intermediate, yields ethane and *s*-propyl cation. Experimental evidence for formation of the less stable 2-C-pentonium (M5) intermediate in superacid media was provided by Olah et al.,¹³ who observed formation of *n*-pentane in the ethylation of propane with C₂H₅F–SbF₅. Of the three processes for which M5 is the common intermediate, the disproportionation reaction that yields methane and 1-butyl cation has the largest equilibrium constant, being the hydride transfer and the dehydrogenation reaction calculated *K_c* values about 4 orders of magnitude lower.

The relative stabilities of TS5, TS6, and TS8 (see Figure 2), which are the transition states for the rate-determining steps of the hydride transfer, disproportionation and dehydrogenation–alkylation reactions, respectively, suggest that the hydride transfer will be by far the fastest reaction. The calculated relative reaction rates $k_{\text{disproportionation}}/k_{\text{hydride-transfer}} = 2 \times 10^{-9}$ and $k_{\text{dehydrogenation}}/k_{\text{hydride-transfer}} = 6 \times 10^{-10}$ are, indeed, very low.

s-C₃H₇⁺ + C₂H₆. It is shown in Figure 3 that, as previously discussed, the 2-methyl-2-C-butionium (M8) formed by addition of ethyl cation to a primary C–H bond of propane yields, by decomposition, *s*-propyl cation and ethane and that the calculated equilibrium constant indicates that this reaction is greatly displaced to the products. Consequently, the sum of the energies of *s*-propyl cation and ethane has been taken as the origin for the relative energies listed in Figure 3. Apart from this hydride transfer reaction, M8 is the common intermediate in four other different processes. One of them is the direct alkylation reaction that in this case yields a branched alkane product, 2-methyl-butane. This product was observed in the study of the ethylation of propane with C₂H₅F–SbF₅ in superacid media.¹³

The disproportionation reaction, which produces methane and 2-butyl cation, can occur through two different reaction paths. The initial transition states in both paths, TS9 and TS10, are energetically equivalent and have a similar structure. However, the presence of one more methyl group bonded to the penta-coordinated carbon atom in TS9 produces some small differences in the optimized values of the several C–H₁ distances. For example, the C₃–H₁ bond in TS9 is slightly more stretched than the C₂–H₁ bond in TS10, while the C₂–H₁ and C₄–H₁ distances in TS9 are shorter than the C₃–H₁ and C₁–H₁ distances in TS10, respectively. In the first reaction path, TS9 directly leads to separated methane and 2-butyl cation, with it being impossible to localize any weak complex between the carbenium ion and the molecule. By following the second reaction path, a new minimum, 3-methyl-1-C-butionium (M9) is localized on the potential energy surface. This structure, which

is 12.7 kcal/mol less stable than M8, has an asymmetrical closed 2e–3c bond between a primary and a methane carbon atoms, and decomposes via transition state TS11 into methane and 2-butyl cation without an activation barrier. In fact, M9 is 0.1 kcal/mol more stable than TS11 unless the ZPE correction is taken into account, in which case the transition state becomes 0.5 kcal/mol more stable than the minimum. The imaginary vibrational mode of 146i cm⁻¹ obtained from the frequency calculation performed for TS11 is related both to the separation of the methane and the butyl fragments and to the migration of the C₅ methyl group from C₃ to C₂.

The last process in which M8 is involved is its dehydrogenation via transition state TS12, yielding as products molecular hydrogen and the branched *t*-C₅H₁₁⁺ cation. This alkylation reaction is specially interesting because it explains the formation of branched products from initial linear reactants.

Since the initial ionic reactant in the processes shown in Figure 3 is not a primary carbenium ion but a more stable secondary one, these reactions are less exothermic than those previously discussed and involve positive activation barriers. It can be seen in Table 5 that the enthalpy values calculated for the different reactions of *s*-propyl cation with ethane are similar, and that the entropy effects slightly favor the disproportionation reaction over the dehydrogenation–alkylation process. The activation barriers for the three different reactions that 2-methyl-2-C-butionium (M8) cation can undergo are quite similar, and therefore the calculated relative rate constants, $k_{\text{disproportionation(a)}}/k_{\text{dehydrogenation}} = 0.3$ and $k_{\text{disproportionation(b)}}/k_{\text{dehydrogenation}} = 0.2$ indicate that the three processes are equally fast.

s-C₃H₇⁺ + C₃H₈. Addition of *s*-propyl cation to a primary or to a secondary C–H bond of propane results in formation of 2-methyl-2-C-pentonium (M10 in Figure 4) and 2,3-dimethyl-2-C-butionium (M12 in Figure 5) carbonium ions, respectively. Like in the C₅H₁₃⁺ system, the different nature of the carbon atoms involved in the nonclassical 2e–3c bonds formed is reflected in the optimized geometries and in the stability of both structures. The primary–secondary C–H–C bond in M10 is asymmetrical (see Table 3) and more acute ($\angle\text{C}_1\text{–H}_1\text{–C}_4 = 161.9^\circ$) than the secondary–secondary bond in M12 ($\angle\text{C}_1\text{–H}_1\text{–C}_4 = 170.4^\circ$), and the difference in energy between both minima is of 6.2 kcal/mol. It is important to note the excellent agreement found between the calculated relative energy of M12 with respect to separated *s*-C₃H₇⁺ + C₃H₈, –12.9 kcal/mol, and the gas-phase experimental value of –13.6 kcal/mol reported by Sunner et al.³⁸

The reaction paths for which the 2-methyl-2-C-pentonium cation (M10) is the common intermediate are depicted in Figure 4. No hydride transfer reaction has been considered in this case, since the process would imply the energetically disfavored transfer from a primary to a secondary carbon atom. The product of the direct alkylation reaction, formed by deprotonation of the C–H–C bond, is in this case a branched alkane, 2-methyl-pentane. A high amount of this species was detected by Olah et al.¹⁸ among the products of the reaction of C₃H₇F–SbF₅ with propane in SO₂ClF/SO₂ media.

M10 is involved in two different disproportionation reactions, one of them yielding methane and the linear 2-pentyl cation (C1 + C5) and the other one yielding ethane and 2-butyl cation (C2 + C4). While in the first process M10 directly decomposes into CH₄ and 2-C₅H₁₁⁺ carbenium ion through TS13, in the second one it is initially converted through TS14 into the 4-methyl-2-C-pentonium carbonium ion (M11), which subsequently decomposes into C₂H₆ and 2-C₄H₉⁺ via transition state TS15. The energy difference of almost 3 kcal/mol existing

between TS13 and TS14 reflects small differences in the geometric optimized values given in Table 3. Thus, the C₂–H₁ and C₄–H₁ distances in TS13 are shorter than the C₁–H₁ and C₅–H₁ distances in TS14 both because of the presence of a methyl group bonded to the pentacoordinated carbon atom in TS13 and because of the different nature of the C₁ (secondary) and C₅ (primary) carbon atoms in TS14. Both structures have been characterized by frequency calculations and have been found to have only one imaginary vibration mode, of 918i and 688i cm⁻¹, respectively, associated with the movement of H₁ from one C–C bond to the other one. M11, which has been characterized as a minimum 0.2 kcal/mol less stable than separated reactants, has a nonclassical closed primary–primary 2e–3c C–H–C bond, with a calculated C₄–H₁–C₅ angle value of 145.6°, and nearly equivalent C–H distances. It decomposes via TS15 with a small activation barrier of 4.4 kcal/mol, yielding ethane and 2-butyl cation. The optimized parameters of TS15, listed in Table 3, and the composition of the only imaginary vibration mode of 240i cm⁻¹ obtained from the frequency calculation indicate that the process implies simultaneous separation of the ethane and butyl fragments and migration of a methyl group from C₁ to C₄. Finally, M10 can undergo dehydrogenation through TS16 yielding hydrogen gas and the alkylated product, the tertiary 2-methyl-2-pentenium carbenium ion.

Figure 5 shows the four reactions in which the 2,3-dimethyl-2-C-butenium cation (M12) formed by addition of *s*-C₃H₇⁺ to a secondary C–H bond of propane is involved. Like in the other systems studied, M12 can (a) give its proton back to the catalyst yielding the branched 2,3-dimethylbutane as the direct alkylation product, (b) decompose again into propane and *s*-propyl cation resulting in hydride transfer, (c) if the bridged proton moves from the central C–C bond to an outer one via TS17, it can decompose into methane and 3-methyl-2-butenium carbenium ion, and (d) dehydrogenate through TS18 yielding hydrogen and the tertiary 2,3-dimethyl-2-butenium carbenium ion.

Experimental evidence for the occurrence of all these reactions in superacid media was provided by the previously mentioned study of Olah et al.¹⁸ Besides the direct alkylation products 2-methylpentane and 2,3-dimethylbutane, they detected hydrogen produced by the dehydrogenation–alkylation reactions, and small amounts of methane and ethane formed in the disproportionation processes.

It can be seen in Table 5 that the two different dehydrogenation reactions are exothermic by 9 kcal/mol, but since they imply an important entropy loss, the calculated equilibrium constants are low, $\sim 5 \times 10^2$. The exothermicity of the disproportionation reaction that yields ethane and 2-C₄H₉⁺ carbenium ion is lower, but its calculated equilibrium constant is comparable to that of the dehydrogenation reaction. The most favored processes from a thermodynamic point of view are the disproportionation reactions in which methane and C₅H₁₁⁺ carbenium ions are formed.

To obtain kinetic information, we have calculated the relative reaction rates of the different processes that have the same carbenium ion as common intermediate. For the reactions involving M10, the calculated values are $k_{\text{disproportionation(CH}_4\text{)}}/k_{\text{dehydrogenation}} = 0.4$, and $k_{\text{disproportionation(C}_2\text{H}_6\text{)}}/k_{\text{dehydrogenation}} = 44$; that is to say, the disproportionation reaction that yields ethane is significantly faster than the two other processes. However, the reactions that occur through formation of M12 are equally fast, with the calculated $k_{\text{disproportionation}}/k_{\text{dehydrogenation}} = 4$.

s-C₃H₇⁺ + *i*-C₅H₁₂. To extend this investigation to reactions of practical interest for the petroleum industry, we have studied

the system formed by interaction of *s*-propyl cation with isopentane, two species that are involved in the mechanism of several acid-catalyzed reactions of hydrocarbons. The isopentane molecule has tertiary, secondary, and two different types of primary C–H bonds, and consequently it can form by interaction with *s*-propyl cation four different carbonium ion intermediates. As could be expected, the most stable is that formed by addition of *s*-C₃H₇⁺ to the tertiary C–H bond of *i*-C₅H₁₂ (M13 in Figure 6). M14, formed by interaction of *s*-C₃H₇⁺ with the secondary C–H bond of *i*-C₅H₁₂, is 6.3 kcal/mol less stable than M13, while the two carbonium ions resulting from addition of *s*-C₃H₇⁺ to the two types of primary C–H bond in *i*-C₅H₁₂, M15 and M17 in Figure 7, are both 6.9 kcal/mol less stable than M14. The optimized bond lengths listed in Table 3 indicate that the nonclassical 2e–3c bond in M13 is almost linear and markedly asymmetrical, due to the different nature of the two carbon atoms involved (secondary vs tertiary). The secondary–secondary C–H–C bond in M14 is slightly more closed than that in M13, but the two C–H calculated distances in the bridge are not completely equivalent because of the different size of the two fragments. In M15 and M17, the bridged hydrogen atom is closer to the primary than to the secondary carbon atoms of the 2e–3c bond, and the calculated C–H–C angles are more acute than those in the two other systems.

Figure 6 shows some of the reactions paths in which M13 and M14 are involved. Both carbonium ions can give, by deprotonation of the C–H–C bond, branched trimethylpentanes as the reaction products of the direct alkylation. They are also the intermediates for the tertiary–secondary and secondary–secondary hydride transfer reactions between isopentane and *s*-propyl cation. The first process yields propane and *t*-amyl cation, which are only 0.9 kcal/mol less stable than M13, while the products of the second process are propane and the less stable secondary *s*-C₅H₁₁⁺ carbenium ion.

Of the many disproportionation reactions that the C₈H₁₉⁺ carbenium ions can undergo, only those that do not give methane as the saturated product have been studied. In the case of M13, the bridged proton can only move to the C₄–C₅ bond via transition state TS19, yielding ethane and the very stable tertiary 2,3-dimethyl-2-butenium carbenium ion. The optimized bond length values of TS19 listed in Table 4 are very similar to those of TS17 in Table 3, indicating that the addition of a second methyl group to the pentacoordinated carbon atom in these transition states has a smaller effect than the addition of the first methyl group. Since migration of the bridged proton from the C₂–C₄ bond to the C₄–C₅ bond in M14 results in an equivalent system, the transition state for this process has not been calculated. Finally, we have found that M13 and M14 undergo dehydrogenation through transition states TS20 and TS21, respectively, yielding in both cases hydrogen and a tertiary C₈H₁₇⁺ carbenium ion. It can be seen in Figure 6 that TS20 is almost 4 kcal/mol less stable than TS21, probably because of the higher steric hindrance existing in TS20.

Some of the reaction paths in which the two carbonium ion intermediates formed by interaction of *s*-C₃H₇⁺ with the primary C–H bonds of *i*-C₅H₁₂, M15, and M17 are involved are depicted in Figure 7. Since the hydride transfer reaction would imply the energetically disfavored transfer from a primary to a secondary carbon atom, this process has not been considered in these two cases. The saturated alkanes obtained from the direct alkylation reactions are branched dimethylhexanes, and the carbenium ions obtained from the dehydrogenation–alkylation reactions that occur via transition states TS24 and TS26 are tertiary dimethylhexenium cations. However, the most

interesting processes in which M15 and M17 are involved are the two disproportionation reactions that yield in both cases isobutane and 2-butyl cation as products.

As shown in Figure 7, M15 is converted, via transition state TS22, into the 2,5-dimethyl-3-butenium carbonium ion intermediate M16, which in turn decomposes through TS23 with a small activation barrier into isobutane and 2-butyl carbenium ion. The optimized geometry of the pentacoordinated carbon atom in TS22, given in Table 4, is different from that of the other transition states obtained for migration of the bridged proton between two neighboring C–C bonds. The distances from C₄ and from the migrating hydrogen H₁ to C₂ and C₅ are longer than in any other case, while the C₄–H₁ calculated distance, 1.089 Å, is equivalent to that of a normal C–H bond. This geometry of the pentacoordinated carbon atom may be caused both by the absence of methyl groups directly attached to C₄ and by the bulkiness of the two alkyl fragments bonded to it. Despite these geometric differences, the reaction coordinate associated with the only imaginary vibration mode obtained for TS22, of 385i cm⁻¹, corresponds, like in the other cases, to the movement of H₁ from one C–C bond to the other one. The reaction intermediate M16 is 4.4 kcal/mol more stable than the separated reactants and only 4.2 kcal/mol less stable than M15. It has a nonclassical 2e–3c bond between two primary carbon atoms, and consequently, it is almost symmetrical, with a calculated C–H–C angle value of 164.6°. It decomposes via transition state TS23 with a small activation barrier into isobutane and 2-butyl cation, in a process that involves simultaneous separation of the two butyl fragments, shortening of the C₄–H₁ distance, and migration of a methyl group from C₆ to C₅.

The other disproportionation reaction that yields isobutane and 2-butyl carbenium ion starts with conversion of M17 into the stable reaction intermediate M18 through transition state TS25. The optimized geometry of the pentacoordinated carbon atom in TS25 is similar to that in TS22; that is to say, it looks like a methyl group inserted into a C–C bond. The imaginary vibrational mode obtained from the frequency calculation performed for TS25, of 508 cm⁻¹, is also clearly associated with the movement of H₁ between the two neighboring C₂–C₄ and C₄–C₅ bonds. M18 has been characterized as a minimum on the C₈H₁₉⁺ potential energy surface, being 10.6 kcal/mol more stable than separated reactants and also more stable than the M17 reaction intermediate. Since the nature of the two carbon atoms involved in its nonclassical C–H–C bond is different, the bond is not symmetrical and the bridged hydrogen atom is closer to the primary C₄ atom (1.208 Å) than to the secondary C₅ (1.368 Å). M18 finally decomposes into isobutane and 2-butyl cation, which are 5.7 kcal/mol less stable, without activation barrier. It is interesting to note that by following this reaction path in the opposite sense, that is to say, if isobutane and 2-butyl cation are considered as the initial reactants, the reaction is only slightly endothermic and the activation barrier is not too high, 12.6 kcal/mol. Consequently, this mechanism could explain the formation of C5 and C3 products in the reactions of C4 alkanes, as for instance in the alkylation of isobutane with butene.³⁹

From the information summarized in Table 5 it can be deduced that the thermodynamically most favorable reactions between *s*-propyl cation and isopentane are the hydride transfer to give propane and *t*-C₅H₁₁⁺ cation and the disproportionation reaction that yields ethane and the 2,3-dimethyl-2-butenium carbenium ion, with the calculated *K_c* value for the secondary–secondary hydride transfer being 8–9 orders of magnitude

smaller. The dehydrogenation–alkylation reactions, despite being exothermic by ~10 kcal/mol, are thermodynamically disfavored mainly due to entropic effects. The disproportionation reactions that yield isobutane and 2-butyl cation are less exothermic, but the calculated equilibrium constants are of the same order, about 10⁴. Furthermore, since they involve lower activation barriers, their calculated relative rate constants *k*_{disproportionation}/*k*_{dehydrogenation} are high, on the order of 10⁴–10⁵, and consequently it will be possible to observe the formation of C4 products in the reactions of C5 and C3 hydrocarbons.

4. Conclusions

The mechanism of the bimolecular reactions of ethyl cation with ethane and propane, and of *s*-propyl cation with ethane, propane, and isopentane has been investigated by means of density functional theory. It has been found that the interaction of a trivalent carbenium ion with a saturated alkane in the gas phase always results in formation of a stable carbonium ion having a nonclassical two-electron three-center C–H–C bond, and that this carbonium ion is the common intermediate for a number of acid-catalyzed reactions of hydrocarbons such as hydride transfer, alkylation, dehydrogenation, and disproportionation. The equilibrium and relative rate constants for these processes have been calculated by means of the transition state theory (TST).

The C–H–C bonds in these carbonium ion intermediates are more or less symmetrical depending on the nature of the two carbon atoms involved and on a lesser extent on the size of the two alkyl fragments bonded. The order of stability obtained is C_{methane}–H–C_{prim} < C_{prim}–H–C_{prim} < C_{prim}–H–C_{sec} < C_{sec}–H–C_{sec} < C_{sec}–H–C_{tert}, and the increase in stability when passing from a type of bond to the next one is of ~6 kcal/mol in all cases. The bridged proton can migrate between two neighboring C–C bonds yielding another carbonium intermediate which can decompose into a carbenium ion and a saturated alkane of different size, giving rise to a disproportionation process. It can also move out of the C–C bond and either go back to the catalyst giving a saturated alkane or form with another H atom a hydrogen molecule, yielding a trivalent carbenium ion. In both cases, the organic species has the same number of carbon atoms as the sum of the carbon atoms of the initial reactants, and therefore the global process can be considered as an alkylation reaction. The last process for which these carbonium ions are the reaction intermediates is the hydride transfer between saturated alkanes and carbenium ions.

In general, both disproportionation and dehydrogenation reactions are exothermic, but since the second process involves an important entropy loss, the equilibrium constants calculated for the dehydrogenation–alkylation reactions are usually smaller than those obtained for the disproportionation reactions. Besides, they are also kinetically disfavored because they use to involve somewhat higher activation energies. The most interesting conclusion obtained from the study of the reactions of *s*-propyl cation with isopentane is that the disproportionation reactions that yield isobutane and 2-butyl cation have equilibrium constant values on the order of 10⁴ and reaction rate constants higher than those obtained for dehydrogenation; therefore, it will be possible to observe the formation of C4 products in the reactions of C5 and C3 hydrocarbons.

Acknowledgment. The authors thank the Departament de Química Física of the University of Valencia for computing facilities. They thank C.I.C.Y.T. (Project MAT97-1016-CO2-01) and Conselleria de Cultura, Educació i Ciència de la

Generalitat Valenciana for financial support. M.B. thanks the Conselleria de Cultura, Educació i Ciència de la Generalitat Valenciana for a personal grant.

References and Notes

- (1) Olah, G. A.; Prakash, G. K. S.; Sommer, J. *Superacids*; Wiley-Interscience: New York, 1995.
- (2) Talrose, V. L.; Lyubimova, A. K. *Dokl. Akad. Nauk. SSSR* **1952**, 86, 909.
- (3) (a) Field, F. H.; Munson, M. S. B. *J. Am. Chem. Soc.* **1965**, 87, 3289. (b) Field, F. H.; Franklin, J. L.; Munson, M. S. B. *J. Am. Chem. Soc.* **1963**, 85, 3575. (c) Wexler, S.; Hesse, N. *J. Am. Chem. Soc.* **1962**, 84, 3425.
- (4) (a) Hiraoka, K.; Kebarle, P. *Can. J. Chem.* **1975**, 53, 970. (b) Hiraoka, K.; Kebarle, P. *J. Chem. Phys.* **1975**, 63, 394.
- (5) Hiraoka, K.; Kebarle, P. *J. Am. Chem. Soc.* **1976**, 98, 6119.
- (6) (a) Ausloos, P.; Rebert, R. E.; Sieck, L. W. *J. Chem. Phys.* **1971**, 54, 2612. (b) Searles, S. K.; Sieck, L. W.; Ausloos, P. *J. Chem. Phys.* **1970**, 53, 849. (c) Burt, J. A.; Dunn, J. L.; McEwan, M. J.; Sutton, M. M.; Roche, A. E.; Schiff, H. Y. *J. Chem. Phys.* **1970**, 52, 6062.
- (7) (a) Dyczmons, V.; Staemmler, V.; Kutzelnigg, W. *Chem. Phys. Lett.* **1970**, 5, 361. (b) Raghavachari, K.; Whiteside, R. A.; Pople, J. A.; Schleyer, P. v. R. *J. Am. Chem. Soc.* **1981**, 103, 5649. (c) Schleyer, P. v. R.; Carneiro, J. W. M. *J. Comput. Chem.* **1992**, 13, 997 and references therein. (d) Schreiner, P. R.; Kim, S.-J.; Schaeffer, H. F.; Schleyer, P. v. R. *J. Chem. Phys.* **1993**, 99, 3716. (e) Marx, D.; Parrinello, M. *Nature* **1995**, 375, 216.
- (8) (a) Bishof, P. K.; Dewar, M. J. S. *J. Am. Chem. Soc.* **1975**, 97, 2278. (b) Köhler, H. J.; Lischka, H. *Chem. Phys. Lett.* **1978**, 58, 175. (c) Carneiro, J. W. M.; Schleyer, P. v. R.; Saunders, M.; Remington, R.; Schaefer, H. F., III; Rauk, A.; Sorensen, T. S. *J. Am. Chem. Soc.* **1994**, 116, 3483.
- (9) (a) Hiraoka, K.; Mori, T.; Yamabe, S. *Chem. Phys. Lett.* **1993**, 207, 178. (b) Collins, S. J.; O'Malley, P. J. *Chem. Phys. Lett.* **1994**, 228, 246. (c) Collins, S. J.; O'Malley, P. J. *J. Chem. Soc., Faraday, Trans.* **1996**, 92, 4347.
- (10) (a) Mota, C. J. A.; Esteves, P. M.; Ramirez-Solis, A.; Hernandez-Lamonedá, R. *J. Am. Chem. Soc.* **1997**, 119, 5193. (b) Esteves, P. M.; Mota, C. J. A.; Ramirez-Solis, A.; Hernandez-Lamonedá, R. *Top. Catal.* **1998**, 6, 163.
- (11) Hiraoka, K.; Kebarle, P. *Can. J. Chem.* **1980**, 58, 2262.
- (12) Blair, A. S.; Heslin, E. J.; Harrison, A. G. *J. Am. Chem. Soc.* **1972**, 94, 2935.
- (13) Olah, G. A.; DeMember, J. R.; Shen, J. *J. Am. Chem. Soc.* **1973**, 95, 4952.
- (14) Olah, G. A.; Olah, J. A. *J. Am. Chem. Soc.* **1971**, 93, 1256.
- (15) (a) Sommer, J.; Bukala, J.; Hachoumy, M.; Jost, R. *J. Am. Chem. Soc.* **1997**, 119, 3274. (b) Sommer, J.; Bukala, J. *Acc. Chem. Res.* **1993**, 26, 370.
- (16) (a) Siskin, M. *Tetrahedron Lett.* **1978**, 6, 527. (b) Siskin, M. *J. Am. Chem. Soc.* **1976**, 98, 5413.
- (17) Olah, G. A.; Felberg, J. D.; Lammertsma, K. *J. Am. Chem. Soc.* **1983**, 105, 6529.
- (18) Olah, G. A.; Mo, Y. K.; Olah, J. A. *J. Am. Chem. Soc.* **1973**, 95, 4939.
- (19) Olah, G. A.; Schlosberg, R. H. *J. Am. Chem. Soc.* **1968**, 90, 2726.
- (20) Mota, C. J. A.; Nogueira, L.; Kover, W. B. *J. Am. Chem. Soc.* **1992**, 114, 1121.
- (21) Sommer, J.; Hachoumy, M.; Garin, F.; Barthomeuf, D.; Vedrine, J. *J. Am. Chem. Soc.* **1995**, 117, 1135.
- (22) Moore, J. W.; Pearson, R. G. *Kinetics and Mechanisms*; Wiley: New York, 1981.
- (23) (a) Hohenberg, P.; Kohn, W. *Phys. Rev. B* **1964**, 136, 864. (b) Kohn, W.; Sham, L. J. *Phys. Rev. A* **1965**, 140, 1133.
- (24) (a) Parr, R. G.; Yang, W. *Density Functional Theory of Atoms and Molecules*; Oxford University Press: New York, 1989. (b) Dreizler, R. M.; Gross, E. K. U. *Density Functional Theory*; Springer: Berlin, 1990. (c) March, N. H. *Electron Density Theory of Many-Electron Systems*; Academic: New York, 1991. (d) *Density Functional Methods in Chemistry*; Labanowski, J. K.; Andzelm, J. W., Eds.; Springer-Verlag: New York, 1991.
- (25) Becke, A. D. *J. Chem. Phys.* **1993**, 98, 5648.
- (26) Perdew, J. P.; Wang, Y. *Phys. Rev. B* **1992**, 45, 13244.
- (27) Hariharan, P. C.; Pople, J. A. *Chem. Phys. Lett.* **1972**, 16, 217.
- (28) Boronat, M.; Viruela, P.; Corma, A. *J. Phys. Chem. A* **1998**, 102, 9863 and references therein.
- (29) Schlegel, H. B. *J. Comput. Chem.* **1982**, 3, 214.
- (30) Frisch, M. J.; Trucks, G. W.; Schlegel, H. B.; Gill, P. M. W.; Johnson, B. G.; Robb, M. A.; Cheeseman, J. R.; Keith, T.; Petersson, G. A.; Montgomery, J. A.; Raghavachari, K.; Al-Laham, M. A.; Zakrzewski, V. G.; Ortiz, J. V.; Foresman, J. B.; Cioslowski, J.; Stefanov, B. B.; Nanayakkara, A.; Challacombe, M.; Peng, C. Y.; Ayala, P. Y.; Chen, W.; Wong, M. W.; Andres, J. L.; Replogle, E. S.; Gomperts, R.; Martin, R. L.; Fox, D. J.; Binkley, J. S.; DeFrees, D. J.; Baker, J.; Stewart, J. P.; Head-Gordon, M.; Gonzalez, C.; Pople, J. A. *Gaussian 94*, revision B.1; Gaussian: Pittsburgh, PA, 1995.
- (31) Frash, M. V.; Solkan, V. N.; Kazansky, V. B. *J. Chem. Soc., Faraday Trans.* **1997**, 93, 515.
- (32) Kristyan, S.; Pulay, P. *Chem. Phys. Lett.* **1994**, 229, 175.
- (33) Hofmann, J. E.; Schriesheim, A. *J. Am. Chem. Soc.* **1962**, 84, 953.
- (34) (a) Koch, W.; Liu, B.; Schleyer, P. v. R. *J. Am. Chem. Soc.* **1989**, 111, 3479. (b) Koch, W.; Schleyer, P. v. R.; Buzek, P.; Liu, B. *Croat. Chem. Acta* **1992**, 65, 655.
- (35) Olah, G. A.; Halpern, Y.; Shen, J.; Mo, Y. K. *J. Am. Chem. Soc.* **1973**, 95, 4960.
- (36) Guisnet, M.; Gnep, N. S. *Appl. Catal. A: General* **1996**, 146, 33 and references therein.
- (37) Sieber, S.; Buzek, P.; Schleyer, P. v. R.; Koch, W.; Carneiro, J. W. M. *J. Am. Chem. Soc.* **1993**, 115, 259.
- (38) Sunner, J. A.; Hirao, K.; Kebarle, P. *J. Phys. Chem.* **1989**, 93, 4010.
- (39) (a) Stöcker, M.; Mostad, H.; Karlsson, A.; Junggreen, H.; Hustad, B. *Catal. Lett.* **1996**, 40, 51. (b) Cardona, F.; Gnep, N. S.; Guisnet, M.; Szabo, G.; Nascimento, P. *Appl. Catal. A: General* **1995**, 128, 243. (c) Corma, A.; Martinez, A.; Martinez, C. *J. Catal.* **1994**, 146, 185.